

PISC III RESULTS ON ACTION 3 "NOZZLES AND DISSIMILAR WELDS"

PH. DOMBRET
AIB-Vinçotte
R&D Department
Avenue du Roi 157
B-1060 Brussels
Belgium

ABSTRACT. Action 3 was initiated in 1986, in the framework of the PISC III programme [1], to evaluate the actual NDE capability for the structural integrity assessment of safe-ends in power plants.

Applying the methodology developed in PISC I and PISC II, Round-Robin Trials (RRT) were organized on the basis of test assemblies representative of BWR and PWR designs, with the objective of identifying effective examination methods, particularly for in-service inspection, and of informing subsequently Codes and Standards organizations of the outcomes.

The features of the assemblies allow to evaluate the inspection performances on reactor pressure vessel safe-end welds, as well as on PWR steam generator and surge line dissimilar metal welds. The attention of the reader is drawn however on the fact that, when conclusions on the NDT capability in industrial conditions are drawn from this exercise, the validity of the comparison must be carefully verified.

The following reviews briefly the organization and integrates the main outcomes of PISC Action 3. Further details can be found in the dedicated PISC reports [2,3,4,5].

1. Round-Robin Test Specimens

Three specimens were made available for the RRT. As a rule, drawings, materials and manufacturing procedures typical of the nuclear industry were used for the fabrication; some exceptions, that may have an impact on the inspection performance, are highlighted below. All nozzle ends were stainless steel clad and Inconel buttered, and all dissimilar metal welds were made from Inconel.

Assembly 20 (Fig. 1) was based on a BWR pressure vessel shell containing two recirculation system inlet nozzles. An Inconel safe-end and a portion of carbon steel pipe was welded, with Inconel, on both nozzles, which are referred to as 21 and 22. As it turned out subsequently, the nozzle ends had been originally prepared by machining through older welds, resulting eventually in the repair-like structure shown in Figure 2.

Assembly 24 is a mockup of a BWR safe-end (Fig. 3). The inside surface of the forged stainless steel safe-end presents a realistic profile, including the thermal sleeve weld. The coolant pipe section was made from wrought stainless steel.

Assembly 25 (Fig. 4) represents a PWR safe-end, welded to a cast stainless steel piping end. However, as a consequence of the unavailability of suitable components, the wall thickness was no more than 40 mm, and a reduction of the inside diameter was present close to the dissimilar metal weld root.

It is obvious that the particular features of the test pieces may have affected incidentally some examination performances. Nevertheless, care was taken during data analysis to cancel the influence of such singularities, and there should be no remaining doubt that the overall conclusions reported below reflect the actual capability of safe-end weld inspection.

2. Flaws

A total of 25 flaws had been intentionally introduced in the assemblies : 3 in the thermal sleeve area of Assembly 24, 13 in the dissimilar metal welds, and 9 in the homogeneous welds. As the depth dimensions ranged from 10 to 50% of the wall thickness, only few of them were acceptable according to ASME XI article IWB-3514 [6]. Figure 5 displays their distribution in three assemblies ; no flaw was intentionally introduced in the dissimilar weld nor in the homogeneous weld of Assembly 22.

Most flaws were planar reflectors, located close to the inside surface, and oriented perpendicular to it or parallel to the fusion lines, to simulate service-induced cracks. Also some sub-surface crack-like reflectors and some fabrication flaws, such as slag inclusions, were considered.

Several fabrication processes were used to introduce the flaws. Planar reflectors were obtained either by fine machining and electro-etching, as in many other PISC exercises, or by a complex technique to be performed during the specimen welding [7] ; Figure 6 shows some typical examples. Care was taken to avoid detectable discontinuities of the metallurgical structure in the vicinity of the flaws.

All flaws were fully certified to allow for a reliable assessment of the inspection capability : beside the information resulting from the fabrication process documentation, the replica technique was used where possible, and radiographic examination was carried out under ideal conditions. Eventually, destructive examination discarded any remaining doubt, after the completion of the RRT. Worth noting is the particular attention paid, during specimen destruction, to some areas where different teams had reported false calls.

The certification process revealed additionally a number of unintended manufacturing flaws, mainly in Assemblies 21 and 22. Whereas one of them was barely acceptable, according to the aforesaid ASME XI criteria, most were much smaller. For obvious reasons of feasibility, it was decided not to consider in the evaluation flaws smaller than 1 mm in height, even though they may have borne an influence on the UT results of some teams.

A total of 47 reference flaws was recorded for the evaluation of the inspection data. Their characteristics and distribution make the specimens as a reasonable set for a performance demonstration test.

3. RRT organization

Subsequently to the insertion of plugs in the BWR type assemblies, to prevent access to the inner surface and radiographic examination, the specimens were circulated in 10 countries (Europe, USA & Japan), to let more than 20 teams carry out a blind examination. As a rule, each team was allotted two weeks to complete the measurements on each assembly.

Table 1 summarizes roughly the procedures implemented by the participants. As made explicit in the Table, a couple of them involve radiography or ultrasonic scanning, in immersion, from the inside of the PWR assembly ; all others are based on contact ultrasonic techniques, from the outer surface. The range includes industrial and laboratory methods, and matches the best NDT technology currently available.

TEAM	SCAN	Assembly 24	Assembly 20	Assembly 25
FN	auto	-	-	Immersion CW focusing probes (ID)
FX		-	-	X-Ray
HM	auto	CW, SW	-	-
IK	manual	-	-	ASME procedure
JK	auto	CW, SW	-	Immersion CW SW focusing probes (ID)
LI	auto	-	-	Immersion CW focusing probes (ID)
MH	manual	-	-	CW, SW (OD & ID)
NG	manual	CW, SW, tandem	-	CW, SW
OE	manual	SW, creep waves, mode conversion	CW, SW, creep waves, TOFD, mode conversion	CW, SW, creep waves, TOFD, mode conversion
OF	manual	CW	-	-
PE	manual	Focusing probes	SW, focusing probes	-
QZ	auto	CW, MOST, SLIC	-	-
RY	auto	CW, SW	CW, SW	CW, SW (OD & ID)
RZ	manual	CW, SW	-	-
TX	manual	CW phased array	-	-
UW	manual	CW, creep waves	-	-
VT	auto	CW, SW, TOFD, SAFT	CW, SW, creep waves, TOFD, SAFT	CW, SW, creep waves, TOFD, SAFT
VY	auto	CW, SW	CW, SW, creep waves	CW, SW, creep waves
WT	auto	-	CW & SW LSAFT	CW & SW LSAFT
XR	manual	CW, SW	ASME procedure	ASME procedure
YR	manual	CW, SW, creep waves, mode conversion	CW, SW, creep waves, mode conversion	-
ZQ	auto	CW, X-Ray	-	CW, X-Ray

Table 1 - Procedures used in the Round-Robin Tests

[CW : compression waves ; SW : shear waves ; other abbreviations should be self-explanatory]

4. Data Evaluation

4.1 METHODOLOGY

The data collected from most teams had to be adapted by the PISC Referee Group, to fit in the evaluation scheme. As a consequence, no conclusion should be drawn with regard to the operational reliability of the applied procedures.

The capability assessment work was carried out with the BTB code [8], along the engineering evaluation principles determined in the previous phases of the PISC programme. The variables used hereafter are as follows :

- FDF : proportion of reference flaws that are detected by a team
- CRF : proportion of rejectable defects that are correctly rejected by a team
- CAF : proportion of acceptable flaws that are correctly accepted by a team
- MESZ : mean error of sizing in the depth direction (in mm)
- SESZ : standard deviation of sizing in the depth direction (in mm)

Two new variables have been introduced to quantify the false call rate of teams, i.e. their propensity to report flaw indications where indeed no actual flaw (with sufficient dimensions) exists : FCRD gives the proportion of false calls in the total number of the team findings, FCRR is similar, but takes only rejectable findings and flaws into consideration.

In addition, averaging of a variable is denoted by a leading *M*. More details on those definitions can be found in [9].

4.2 TEAMS PERFORMANCES

Figures 7 to 10 illustrate the results obtained by all participating teams. Only a few of the teams reach a flaw detection frequency of 80%, whereas a significant number of false calls are reported.

Regarding the capability of flaw sizing in the through-wall direction, a slight tendency to oversizing appears, on average, but the standard deviation is comparatively large. The overall dispersion of the sizing error is of the order of ± 5 mm, as illustrated by Figure 11.

As most acceptable flaws were very small, they are more frequently accepted than significant defects are rejected. The correct rejection frequency remains, on average, beneath 70%. As a general rule, high detection rates are obtained at the cost of oversizing, rejection of acceptable flaws, or high false call rates. A couple of teams however succeed in scoring well against all parameters.

Table 2 shows that no significant difference appears between the average results obtained on the dissimilar welds and on the really homogeneous welds of Assemblies 24 and 25. It may be however that the inspection and analysis resources spent by the teams were not equivalent for these different welds.

It should also be observed that the overall capability is lower on Assembly 20. This can be explained by the existence of many natural flaws, the difficulty of implementing advanced

techniques, the shorter time available for each weld, the smaller size of the intended flaws, and the complex structure of the heterogeneous weld.

Assembly	Weld	FDL	CRF	CAF	FCRD	FCRR	MESZ	SESZ
24	AW	0.53	0.53	-	0.32	0.30	1.7	3
	DW	0.64	0.69	1.00	0.35	0.23	0.1	5
21	AW	0.42	0.22	0.61	0.34	0.24	3.8	6
	DW	0.34	0.46	0.87	0.14	0.07	1.5	5
22	AW	0.18	-	0.93	0.36	0.33	2.1	3
	DW	0.23	-	0.86	0.20	0.17	6.6	6
25	AW	0.75	0.61	-	0.17	0.08	-3.5	5
	DW	0.80	0.75	-	0.12	0.04	-2.5	6

Table 2 - Average results on dissimilar metal welds and homogeneous welds, for examinations from the outside surface only

4.3 EXAMINATION PROCEDURE PERFORMANCES

Teams can be grouped in families, on the basis of key features of the procedure they implemented. Such families have been defined to investigate the influence of the procedure sensitivity, i.e. the signal recording threshold, and of the scanning mechanization. Except where specified, only ultrasonic examinations conducted from the outside surface are analyzed in this section. Figure 12 illustrates the average flaw detection and correct rejection performance of the procedure families, versus their false call scores. The overall trends arising from these diagrams are more deeply analyzed in the following.

Table 3 shows an obvious correlation between the inspection sensitivity and its capability : recording at noise level, i.e. with no amplitude threshold, is more efficient than using a threshold in the range of 10 to 25% DAC, whereas recording above 50% DAC is unsatisfactory, except on Assembly 25.

No explicit conclusions can be inferred from a similar comparison between manual scanning and automatic scanning. A more detailed analysis, considering subgroups of teams working in the same sensitivity ranges, leads to believe that no definite impact on the testing capability can be associated with scanning mechanization. Practically, the decision of automating a procedure must probably result from reliability and personnel safety considerations, rather than from capability evaluations.

Family	Assembly	FDI	CRF	CAF	FCRD	FCRR	MESZ	SESZ
Noise level	24	0.73	0.77	1.00	0.35	0.30	1.5	4
	20	0.33	0.65	0.84	0.29	0.24	3.3	7
	25	0.78	0.64	-	0.13	0.08	-2.5	5
10 - 25% DAC	24	0.54	0.59	1.00	0.49	0.38	0.0	5
	20	0.32	0.27	0.78	0.47	0.39	4.0	5
	25	0.82	0.78	-	0.24	0.07	-0.3	6
50% DAC	24	0.34	0.28	1.00	0.28	0.00	-1.3	7
	20	0.18	0.10	1.00	0.17	0.5	-0.5	2
	25	0.73	0.62	-	0.07	0.00	-2.0	5

*Table 3 - Results of Procedure Families
(examinations from outside surface only ; thermal sleeve of Assembly 24 excluded)*

4.4 EXAMINATION TECHNIQUE PERFORMANCES

Few teams provided detailed results for each technique considered in their procedure. Because these results were not processed to reach a final decision on the flaw size, only the detection capability was analyzed, as far as possible. Not surprisingly, the essential contribution of compression wave techniques was observed, but no single technique could equal the results of the full procedure.

Furthermore, two teams provided radiographic inspection results, obviously with no depth sizing, on Assembly 25. The flaw detection capability is similar to the average UT performance, but with a higher false call rate. In addition, it can be noted that the same flaws proved to be difficult for X-ray and ultrasonic testing.

4.5 INFLUENCE OF EXAMINATION SIDE

During the round-robin tests, access was allowed to the inner surface of the PWR-like Assembly 25. Four teams submitted data collected from this side only, and Table 4 compares their average results to those obtained from the outside surface.

However, some bias is introduced in the comparison, as 3 of the 4 procedures applied from the inside were based on immersion focusing transducers : indeed, this procedure family demonstrated its high inspection capability, in spite of the aforesaid wall thickness change in Assembly 25, which penalized particularly its flaw detection performance.

Surface	Weld	FDI	CRF	FCRD	FCRR	MESZ	SESZ
OD	AW	0.75	0.61	0.17	0.08	-3.5	5
	DW	0.80	0.75	0.12	0.04	-2.5	6
ID	AW	0.88	0.69	0.05	0.00	-5.0	3
	DW	0.75	0.70	0.17	0.03	-3.0	3

Table 4 - Average results on Assembly 25, for examinations from either the OD or the ID surface

4.6 INFLUENCE OF FLAW CHARACTERISTICS

Taking all teams in consideration, Figure 13 shows the average probability of detection and of correct rejection, for each flaw, as a function of its depth dimension (in percent of the wall thickness). Distributing flaws among categories, on the basis of their location and morphology, leads to the conclusion that the reflectors located in carbon steel or in wrought austenitic steel, far enough from welds, are much better characterized than those neighbouring or embedded in fused material. Seemingly, flaws extending within the welds or along the safe-end fusion lines appear most difficult.

Furthermore, it turns out from Figure 13 that the detection of reflectors smaller than 2 mm (i.e. about 5% of the wall thickness) lies beyond the reach of today's common technology. This observation is confirmed by additional measurements achieved by some teams after the RRT.

Figure 14 depicts the sizing accuracy as a function of the flaw through-wall extent. Drawing regression lines through the scatter of data leads to the conclusion that the mean error remains constant, whereas the standard deviation evidently increases with the flaw size.

A comparison was attempted between the actual flaw distribution and that reported by a virtual inspector matching the average performance of all teams (Fig. 15). Disregarding the very small flaws, the total number of declared indications is roughly correct ; the actual peak in the range of 25 to 35% of the thickness is only flattened by the flaw sizing error.

Summary

Safe-end welds certainly appear amongst the major concerns of the international NDE community. PISC III Action 3 confirmed the difficulty of their inspection.

Even if the average flaw evaluation capability, as assessed in the exercise, may not match the current expectations, some procedures have demonstrated their ability to detect and size quite accurately service-like flaws in such heterogeneous austenitic structures.

Factors enhancing the inspection results have been identified to permit an improvement of the industrial capability. Among those, the importance of the data recording level was highlighted.

Each of the assemblies is specific, however, with respect to its constitutive materials, geometric design, manufacturing procedure, and flaws. As, in addition, examinations achieved in PISC are most generally not fully representative of field conditions, care should be taken before extrapolating the conclusions of the exercise to practical situations.

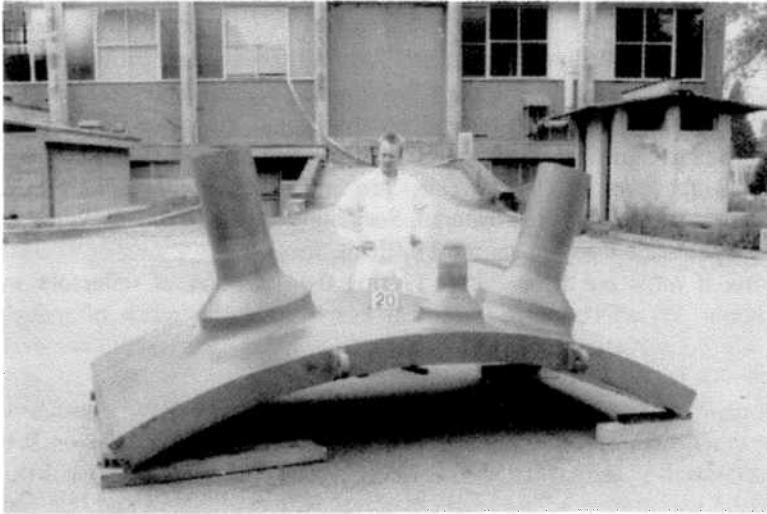


Fig. 1 - Assembly 20 (21 & 22)

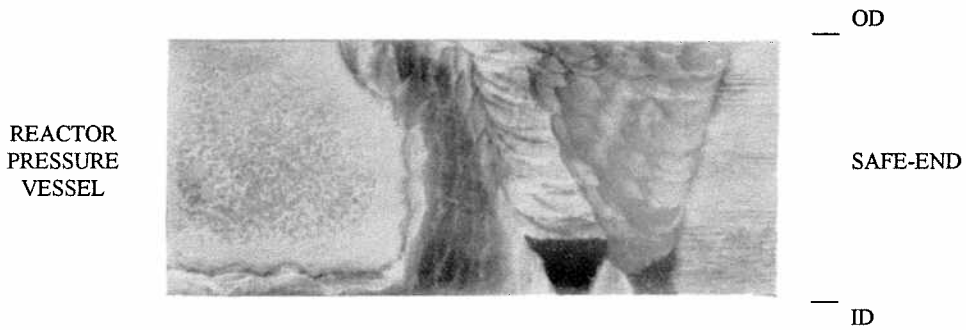


Fig. 2 - Macrograph of the dissimilar metal weld of Assembly 21



Fig. 3 - Assembly 24

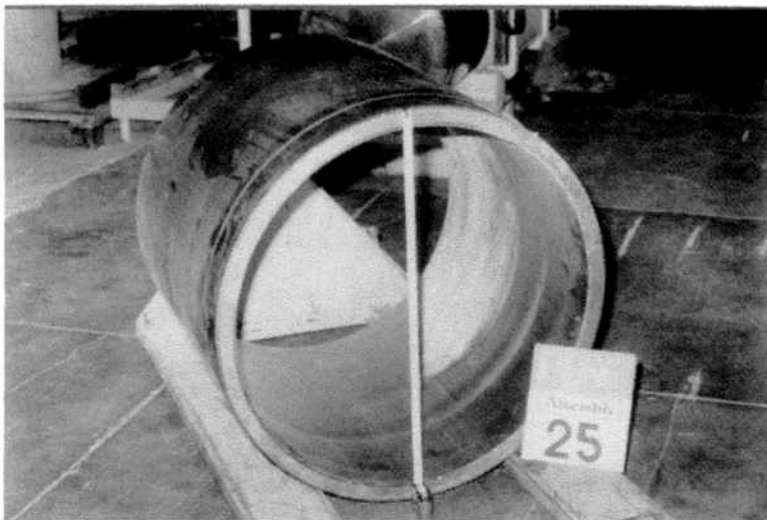


Fig. 4 - Assembly 25

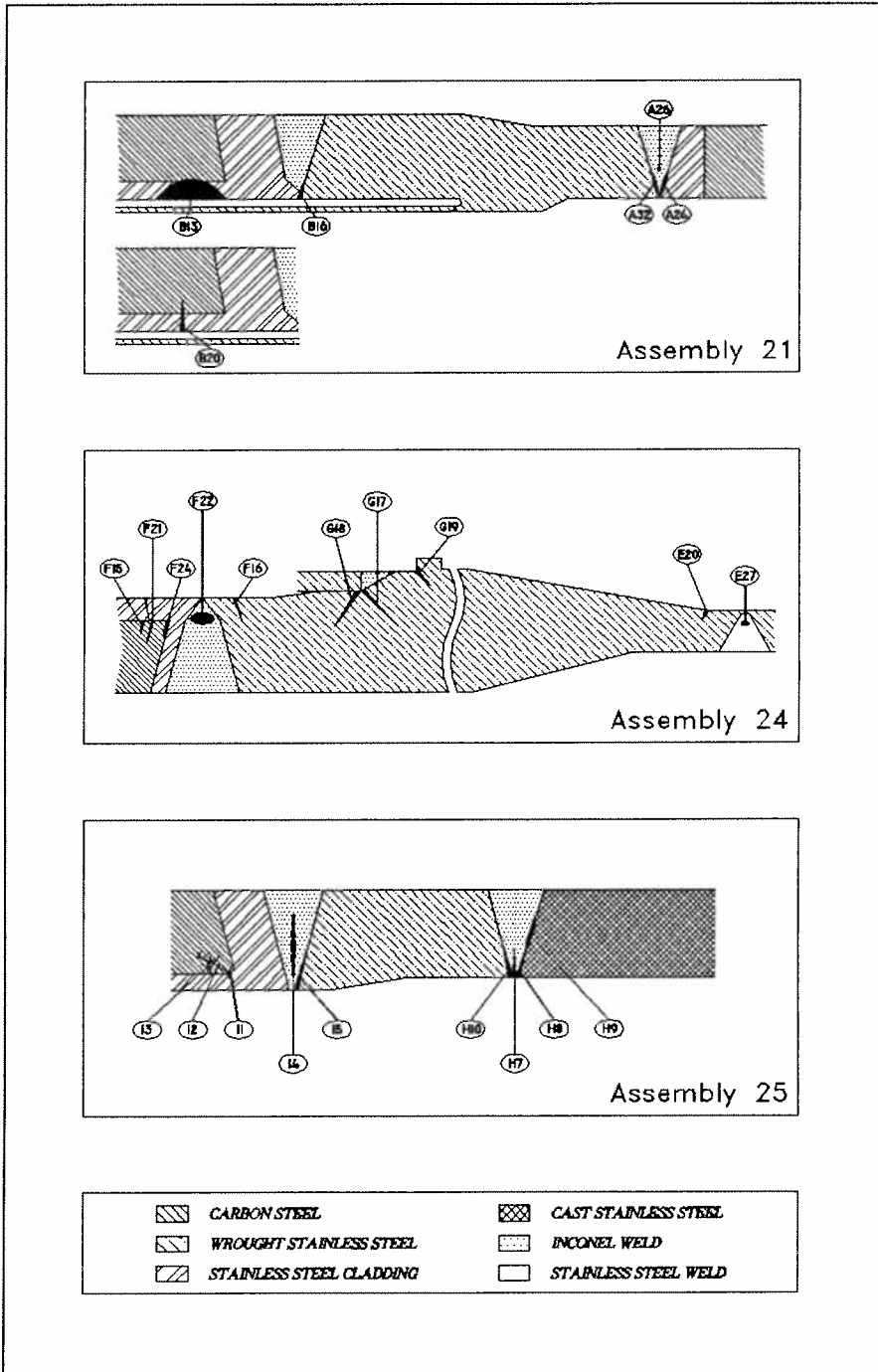
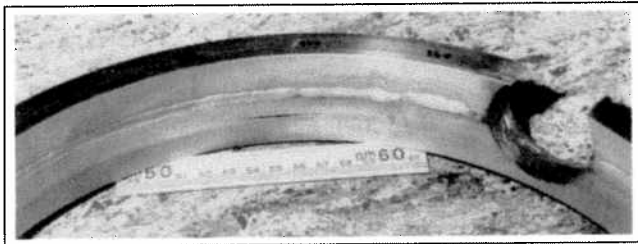
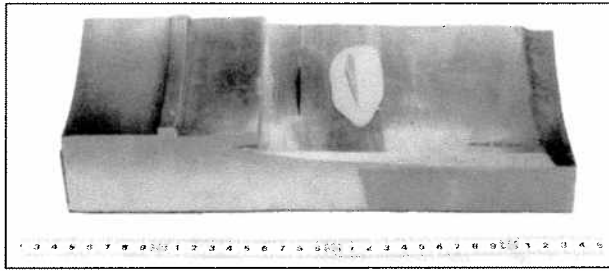


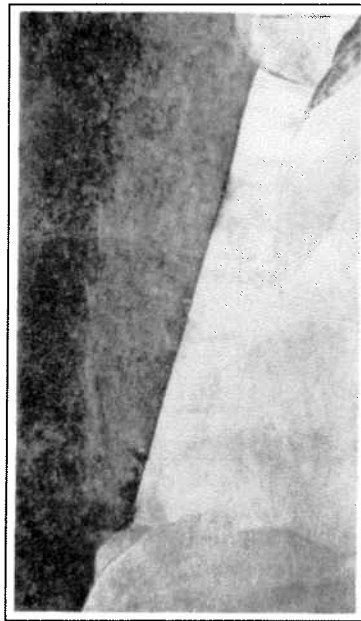
Fig. 5 - Flaw distribution in the 3 assemblies



a. machined flaws



b. Flaw I5 (Assembly 25)



c. Flaw H9 (Assembly 25)

Fig. 6 - Typical flaws

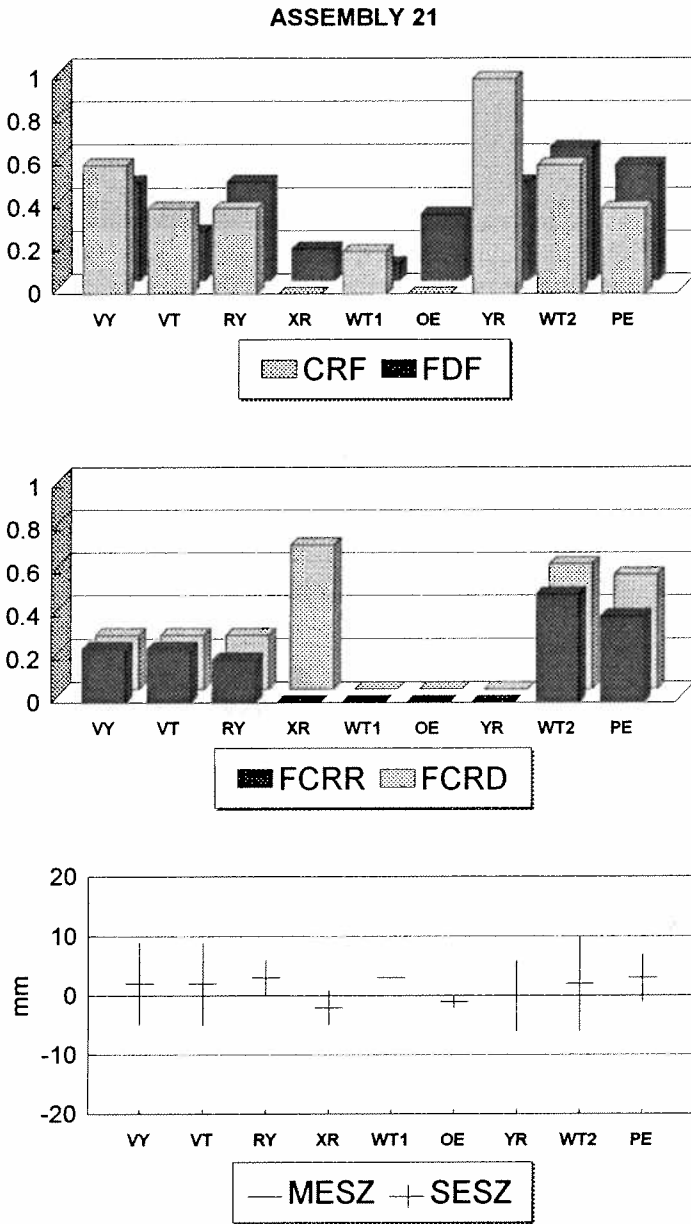


Fig. 7 - Results of all teams on Assembly 21

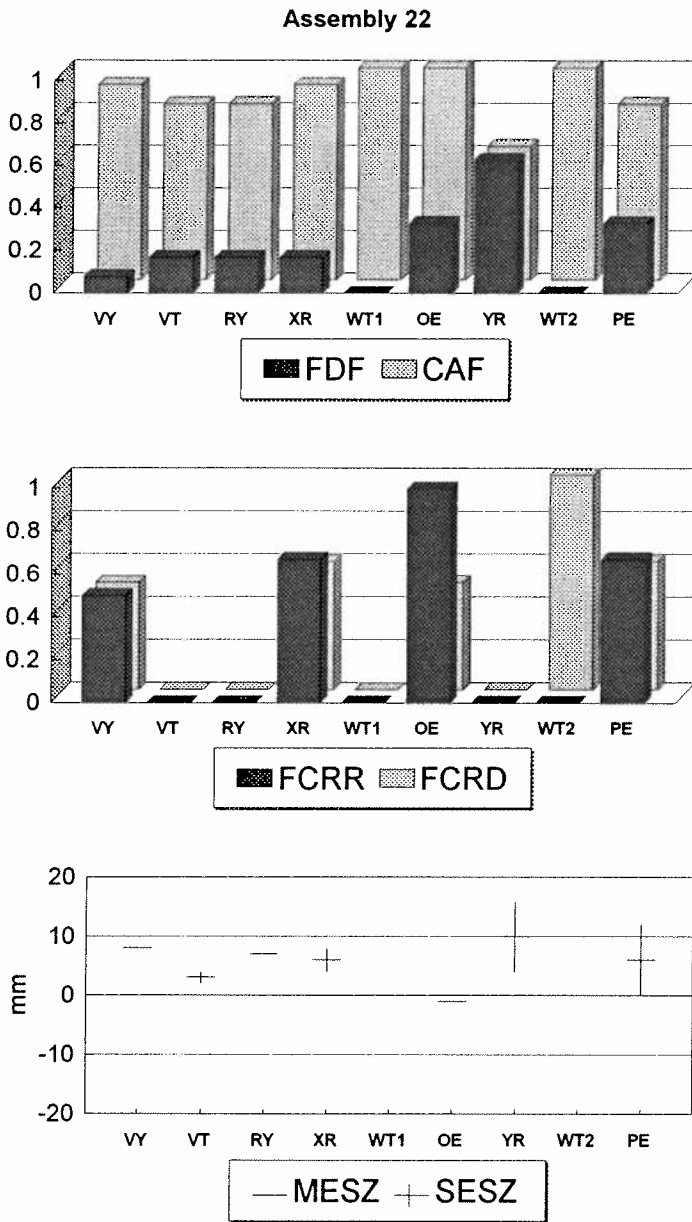


Fig. 8 - Results of all teams on Assembly 22

Assembly 24

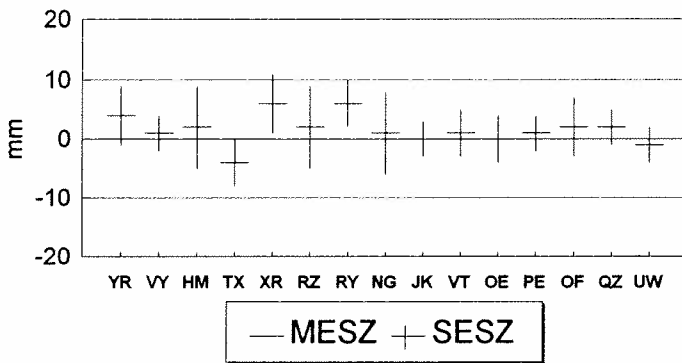
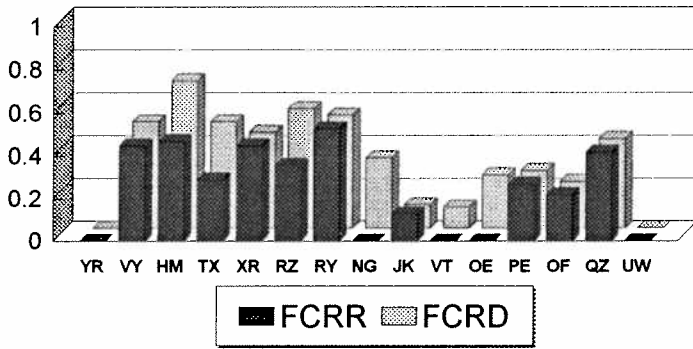
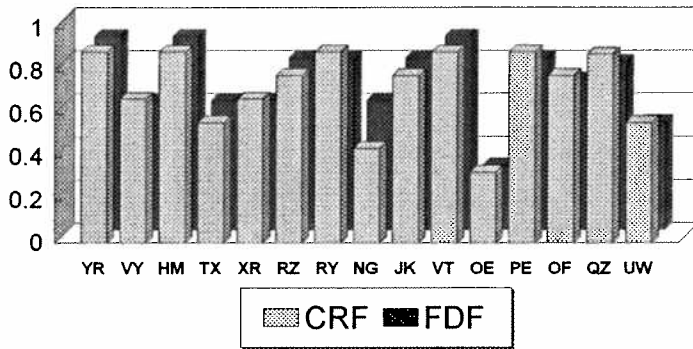


Fig. 9 - Results of all teams on Assembly 24

Assembly 25

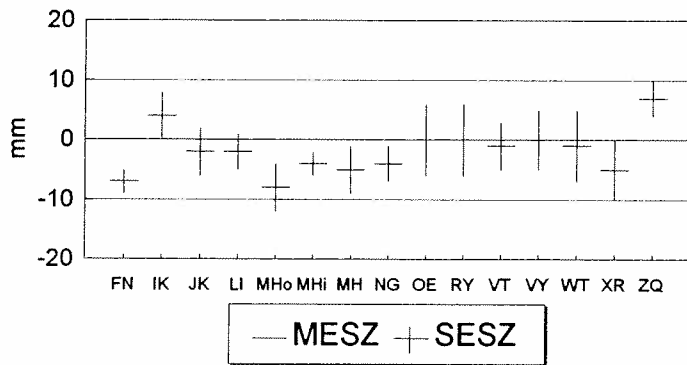
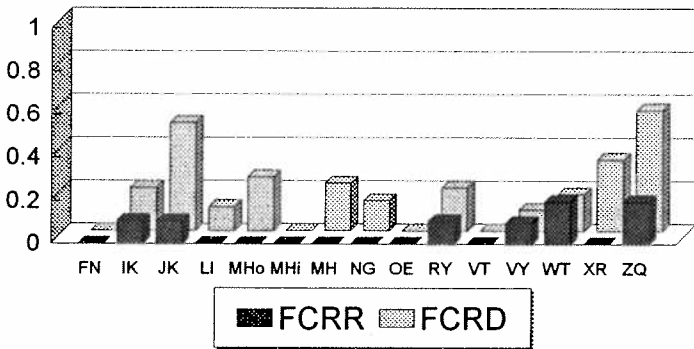
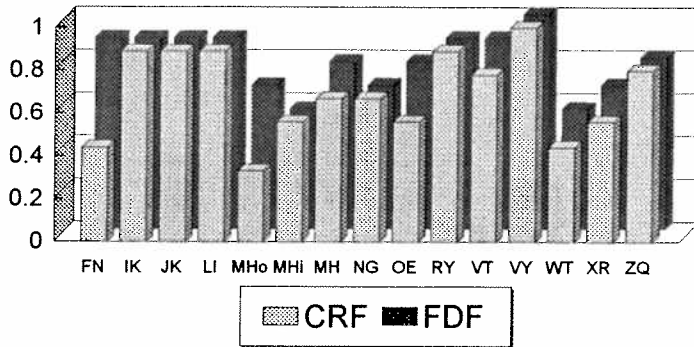


Fig. 10 - Results of all teams on Assembly 25

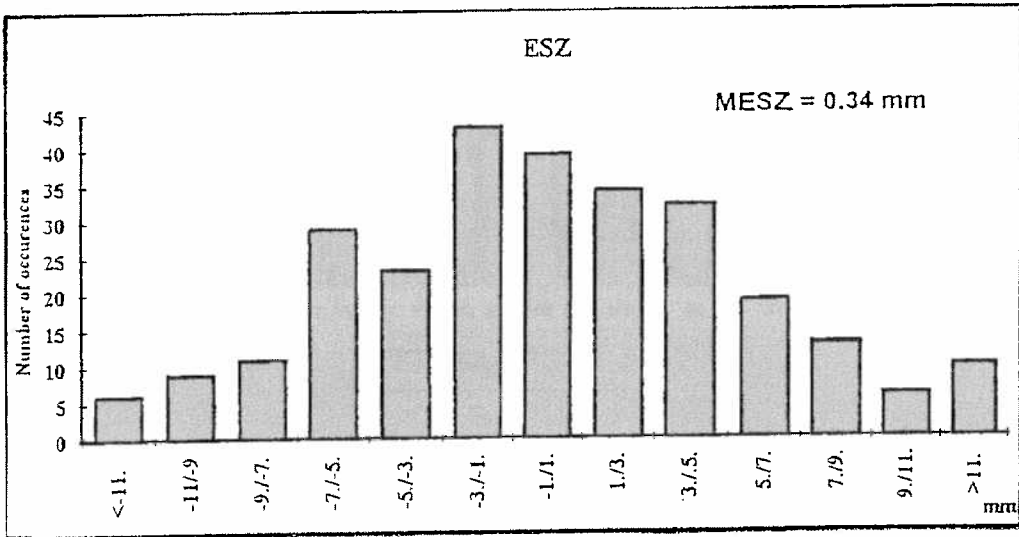


Fig. 11 - Distribution of the sizing error (all assemblies)

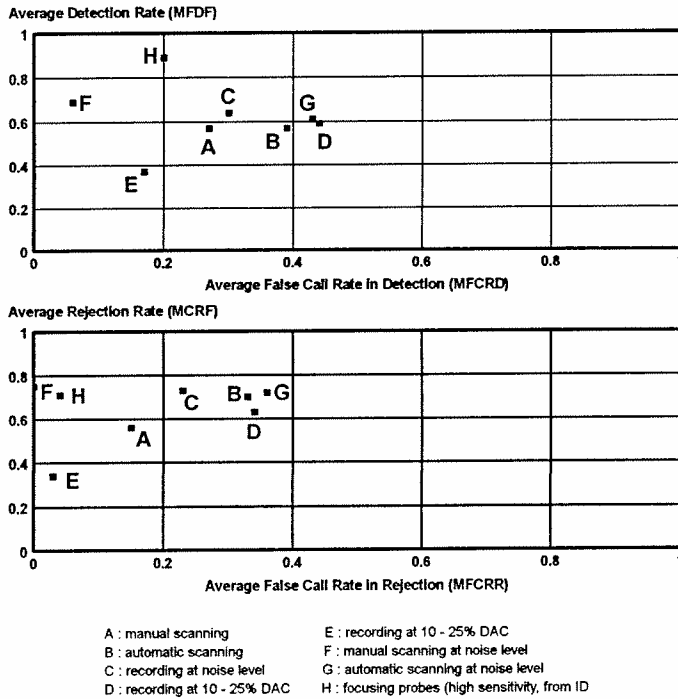


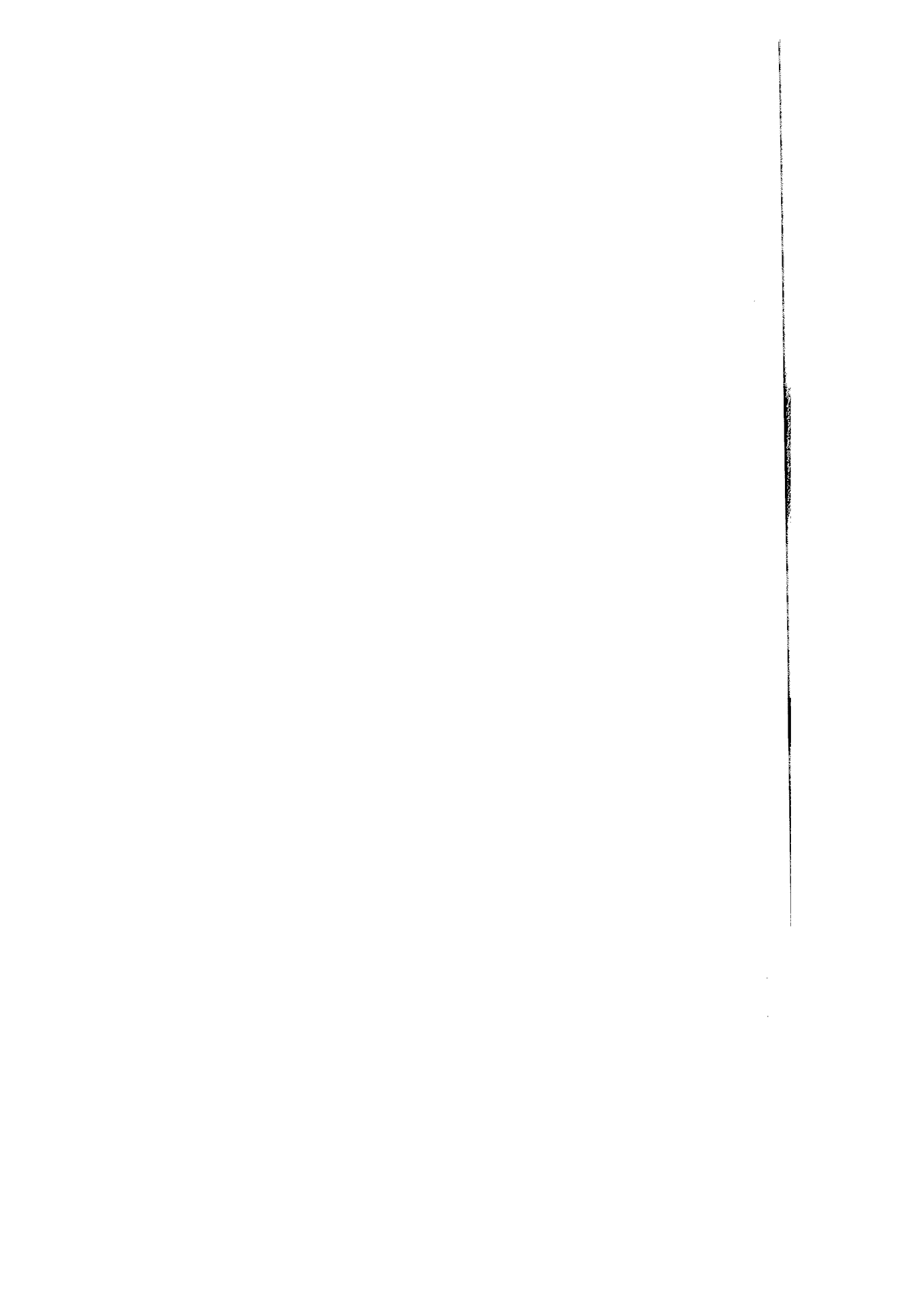
Fig. 12 - Results of inspection procedure families

Acknowledgements

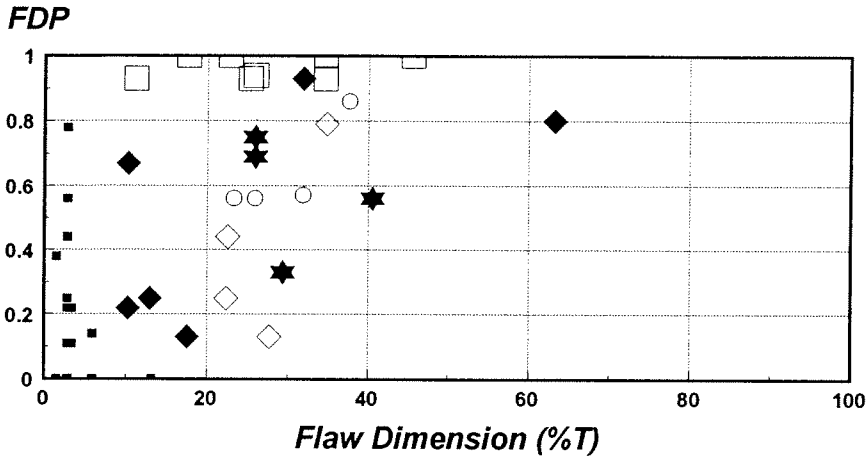
The evaluation work was achieved by the Institute for Advanced Materials of the CEC Joint Research Centre, under the guidance of the Data Analysis Group members (Ph. Dombret, AIB-Vinçotte ; F. Champigny, EDF ; M. Gribi, Sulzer Innotec ; K. Högberg, TRC ; A.J. Willetts, NII), whose competence and involvement was greatly appreciated.

References

- [1] PISC Report n°17 - Summary of the Three Phases of the PISC Programme - CEC JRC, OECD NEA/CSNI, 1992
- [2] PISC Report n°20 - Evaluation of the Inspection Results of the Safe-End Areas of PISC III Assembly n°20 - CEC JRC, OECD NEA/CSNI
- [3] PISC Report n°24 - Evaluation of the Inspection Results of the Safe-End Areas of PISC III Assembly n°24 - CEC JRC, OECD NEA/CSNI
- [4] PISC Report n°25 - Evaluation of the Inspection Results of the Safe-End Areas of PISC III Assembly n°25 - CEC JRC, OECD NEA/CSNI
- [5] PISC Report n°22 - Integrated Evaluation of the Inspection Results of the Safe-End Areas of PISC III Assemblies n°20, 24 and 25 - CEC JRC, OECD NEA/CSNI
- [6] ASME Boiler and Pressure Vessel Code, Section XI
- [7] J.A. Diez-Aja - Implanting of realistic artificial defects in test assemblies - Reactor Safety Research, edited by W. Krischer, Elsevier Applied Science, 1990
- [8] Short Description of BTB Code - PISCDOC (91)20 - June 1991
- [9] PISC III Rules for the Evaluation of the RRT Results - PISCDOC (87)9, 3rd revision - May 1991



Flaw Detection Probability



Flaw Correct Rejection Probability

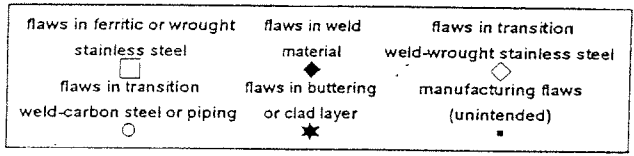
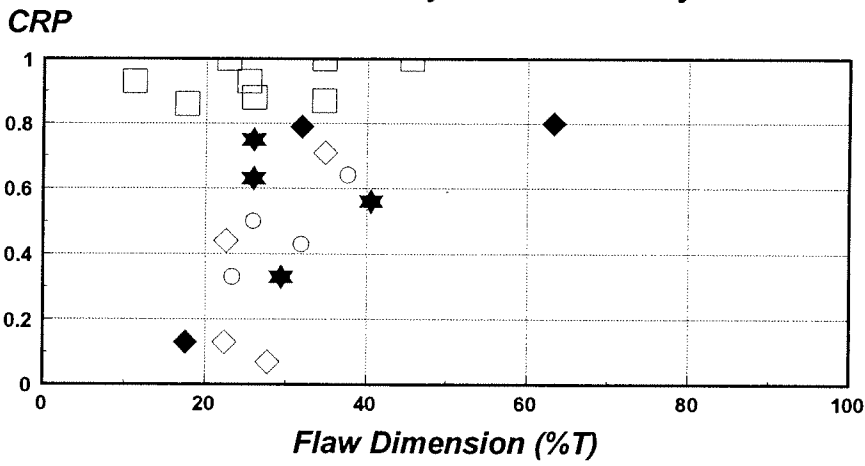


Fig. 13 - Flaw detection and rejection probability

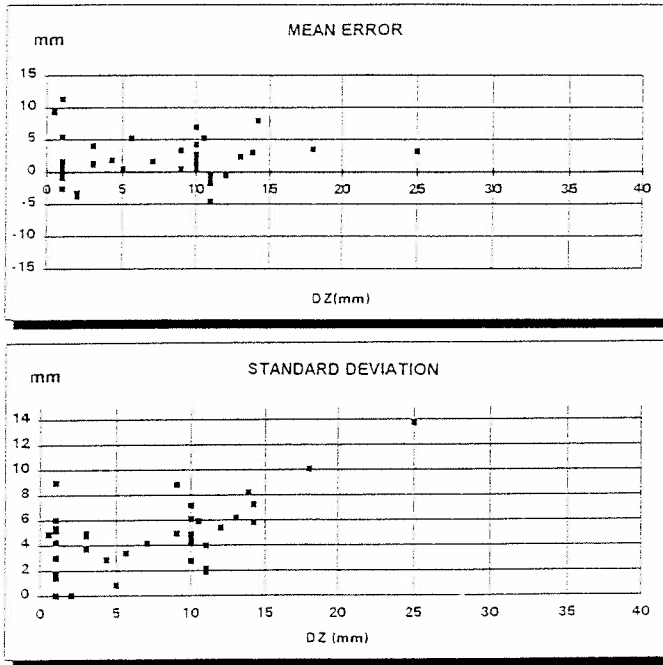


Fig. 14 - Mean error of sizing and standard deviation of each flaw

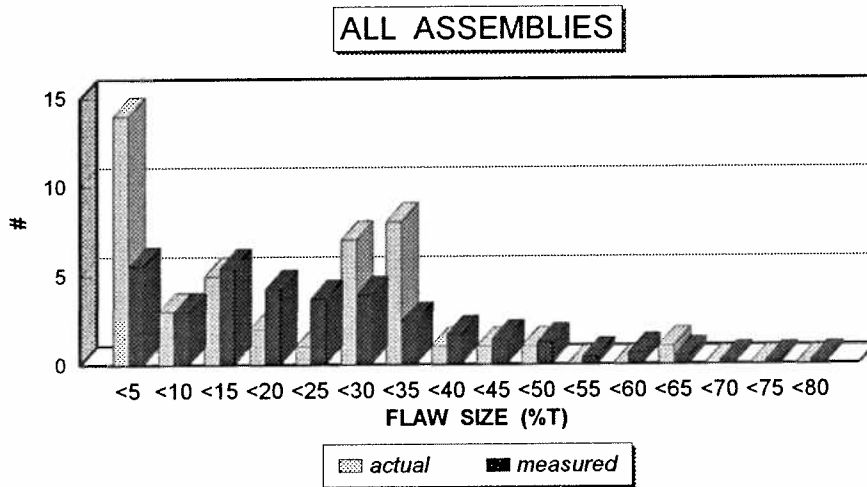


Fig. 15 - Flaw dimension distribution